Assembly of Plant *Shaker*-Like K_{out} Channels Requires Two Distinct Sites of the Channel α-Subunit

Ingo Dreyer,*†‡ Fabien Porée,*†‡ Antje Schneider,†‡ Jessica Mittelstädt,† Adam Bertl,§ Hervé Sentenac,* Jean-Baptiste Thibaud,* and Bernd Mueller-Roeber†‡

*Biochimie et Physiologie Moléculaires des Plantes, UMR 5004, Agro-M/CNRS/INRA/UM2, F-34060 Montpellier Cedex 1, France; †Universität Potsdam, Institut für Biochemie und Biologie, Abteilung Molekularbiologie, D-14476 Golm/Potsdam, Germany; ‡Max-Planck Institute of Molecular Plant Physiology, Cooperative Research Group, D-14476 Golm/Potsdam, Gemany; and §Botanisches Institut I, Universität Karlsruhe, 76128 Karlsruhe, Germany

ABSTRACT SKOR and GORK are outward-rectifying plant potassium channels from *Arabidopsis thaliana*. They belong to the *Shaker* superfamily of voltage-dependent K^+ channels. Channels of this class are composed of four α-subunits and subunit assembly is a prerequisite for channel function. In this study the assembly mechanism of SKOR was investigated using the yeast two-hybrid system and functional assays in *Xenopus* oocytes and in yeast. We demonstrate that SKOR and GORK physically interact and assemble into heteromeric K_{out} channels. Deletion mutants and chimeric proteins generated from SKOR and the K_{in} channel α-subunit KAT1 revealed that the cytoplasmic C-terminus of SKOR determines channel assembly. Two domains that are crucial for channel assembly were identified: i), a proximal interacting region comprising a putative cyclic nucleotide-binding domain together with 33 amino acids just upstream of this domain, and ii), a distal interacting region showing some resemblance to the K_T domain of KAT1. Both regions contributed differently to channel assembly. Whereas the proximal interacting region was found to be active on its own, the distal interacting region required an intact proximal interacting region to be active. K_{out} α-subunits did not assemble with K_{in} α-subunits because of the absence of interaction between their assembly sites.

INTRODUCTION

Potassium (K^+) is the most abundant cation in plants and is involved in many cellular processes. The uptake of K^+ and its redistribution throughout the plant is accomplished by a variety of membrane transport systems (for reviews see Dreyer et al., 1999, 2002; Maser et al., 2001; Very and Sentenac, 2002, 2003). Most of the present knowledge in this field concerns K^+ channels of the *Shaker* type, which have been shown to form the major (voltage-gated) K^+ conductance in several cell types and to play physiologically important roles in various K^+ transport processes (Pilot et al., 2003a).

Like their animal relatives, plant *Shaker*-like K^+ channels are composed of four α-subunits. Each subunit displays a hydrophobic core comprising six transmembrane segments, named S1–S6, and a pore forming loop, named P, between S5 and S6. A putative cyclic nucleotide-binding domain (cNBD) is present downstream of the hydrophobic core. Based on phylogenetic analyses it has been shown that the family of plant *Shaker*-like K^+ channels can be subdivided into five subfamilies (Pilot et al., 2003b). However, at the functional level this segregation simplifies to three subfamilies: inwardly rectifying K_{in} channels mediating potassium uptake, outwardly rectifying K_{out} channels mediating potassium release, and weakly rectifying K_{weak} channels thought to be able to mediate both K^+ uptake or release depending on the local K^+ electrochemical gradients. In the model plant *Arabidopsis thaliana*, the nuclear genome comprises a total of nine genes coding for *Shaker*-like K^+ channels. Among those, seven have functionally been characterized: four K_{in}, i.e., KAT1, KAT2, AKT1, and SPIK; one K_{weak}, i.e., AKT2; and two K_{out} channels, i.e., SKOR and GORK (Very and Sentenac, 2002, 2003).

In the case of *Shaker*-type K^+ channels, tetramerization of α-subunits is a prerequisite for pore formation and electric activity (Dreyer et al., 1997). The availability of α-subunits, and the amount of α-subunits assembled into a functional tetrameric complex, is of central cellular importance. The assembly process itself may be regulated according to the physiological needs of the cell. Identifying the protein domains in K^+ channel α-subunits that trigger and contribute to channel assembly is therefore an important task. Previously, various research groups have investigated the assembly of plant K_{in} channels, but not of K_{out} channels. Initial information in this field was provided by three studies in 1997. Using KAT1 as a model, Marten and Hoshi (1997) showed through deletion experiments that the far C-terminus of the α-subunit is not essential for functional channel assembly. KAT1 was still functional when its C-terminal part downstream of the putative cyclic nucleotide-binding domain was deleted. Further deletions toward the N-terminus of the protein resulted in nonfunctional channels (Marten and Hoshi, 1997). In a second study, using a biochemical approach, Daram et al. showed that the C-terminus of AKT1 has the capability to form a homotetrameric

Submitted November 25, 2003, and accepted for publication May 5, 2004.

Address reprint requests to Ingo Dreyer, Universität Potsdam, Institut für Biochemie und Biologie, Abteilung Molekularbiologie, Karl-Liebknecht-Strasse 24-25, Haus 20, D-14476 Golm/Potsdam, Germany. Fax: 49-331-977-2512; E-mail: dreyer@rz.uni-potsdam.de.

0006-3495/04/08/858/15 $2.00

doi: 10.1529/biophysj.103.037671

complex (Daram et al., 1997). Subsequent yeast two-hybrid interaction tests using eight different constructs generated from the AKT1 C-terminus provided more detailed information about protein regions involved in the aggregation process. An internal fragment of 145 amino acid residues, comprising the putative cyclic nucleotide-binding domain, was shown to display self-interaction, suggesting a role in subunit assembly. However, evidence was provided that this region was not the only determinant of C-terminus interaction because C-terminal fragments lacking it still aggregated with others. An additional type of interaction between a domain at the far end of the C-terminus and a region located between transmembrane segment S6 and the putative cyclic nucleotide-binding domain was proposed. In addition to these results, a third type of interaction has been reported. Whereas the far end of the C-terminus (the so called K_{HA} domain) failed to self-interact in the case of AKT1 (Daram et al., 1997), Erhardt et al. observed self- and cross-interactions between the K_{HA} domains of three different K_{in} channels from potato (Ehrhardt et al., 1997).

Plant *Shaker*-type K_{in} α-subunits have not only the capability to homotetramerize. Importantly, different types of K_{in} α-subunits assemble, in different combinations, into heteromeric, electrically fully active K_{in} channels when expressed in heterologous systems (Dreyer et al., 1997), adding a further potential level of regulation, that in part may rely on the interaction domains present in these proteins. Recently, an electrophysiological study on the potato K_{in} channels SKT1 and KST1 related another domain, named K_T, and located directly upstream of the K_{HA} domain, with channel heterotetramerization (Zimmermann et al., 2001).

The above reports provide some aspects about the assembly of plant *Shaker* K_{in} channels. However, the picture is still vague and in part contradictory. Furthermore, none of these studies correlated physical interactions between protein regions with their functional consequences for channel assembly.

This report investigates the assembly behavior of the plant K_{out} channels SKOR and GORK (Gaymard et al., 1998; Ache et al., 2000). Using the yeast two-hybrid system and two different heterologous expression systems (*Xenopus* oocytes and yeast) suitable for functional analyses, we studied intersubunit physical interactions and analyzed their importance for functional channel assembly. We demonstrate that in plant K_{out} channels two distinct domains located in the cytoplasmic C-terminal part of the protein are essential for channel assembly.

MATERIALS AND METHODS

Recombinant DNA techniques

Standard methods of plasmid DNA preparation, PCR, restriction enzyme analysis, agarose gel electrophoresis, and bacterial transformation were applied (Ausubel et al., 1993). Chimeras and mutants were created by PCR-based techniques and with the pAlter mutagenesis system (Promega, Charbonnières, France). Further detailed information concerning the 77 constructs tested in this study will be provided upon request.

Electrophysiology

Xenopus oocytes were injected with a volume of 40 nl of cRNA mixtures. Mixtures indicated in the figure legends were prepared from 1 μg/μl cRNA stock solutions. Control oocytes were injected with 40 nl of deionized water. Two-electrode voltage-clamp experiments were carried out as previously described (in France according to Lacombe and Thibaud, 1998; in Germany according to Becker et al., 1996). External standard solution was composed of 10 mM KCl, 90 mM NaCl, 1 mM $CaCl_2$, 2 mM $MgCl_2$, 10 mM Tris/MES pH 7.0. Patch-clamp experiments on yeast protoplasts were carried out as recently described by Bertl et al. (1998). Standard pipette solution contained 175 mM KCl, 4 mM $MgCl_2$, 4 mM K-ATP, 1 mM EGTA, 152 μM $CaCl_2$, adjusted to pH 7.0 with KOH. Extracellular solution contained 150 mM KCl, 10 mM $CaCl_2$, 5 mM $MgCl_2$, buffered to pH 6.5 with MES/Tris. Measurements were carried out from a holding potential of -40 mV. Currents were evoked by 2.5-s activating voltage pulses from $+100$ mV to -200 mV (20-mV steps).

Yeast complementation

The yeast strain Wagf2 (*ade2-101*; *his3-11,15*; *leu2-3,112*; *trp1-1*; *ura3-1*; *trk1*Δ*::LEU2*; *trk2*Δ*::TRP1*; *can*^{r}) (Ros et al., 1999) is deficient for K^+ uptake and displays reduced growth in physiological conditions, when the external concentration of K^+ is low ($\sim$5 mM). It was used for complementation tests together with two yeast expression plasmids: the multicopy plasmid pFL61 (*URA3* as a selection marker) (Minet et al., 1992), and the centromeric plasmid pFL38His-PGK (*HIS3* as a selection marker) (Ros et al., 1999). Selection minimal medium was based on a synthetic arginine/phosphate medium (Rodriguez-Navarro and Ramos, 1984) containing 2% glucose, 10 mM L-arginine, 150 μM adenine, 2 mM $MgSO_4$, 200 μM $CaCl_2$, 13 μM FeNa-EDTA, 8 μM H_3BO_3, 0.25 μM $CuSO_4$, 0.6 μM KI, 2.7 μM $MnSO_4$, 1 μM Na_2MoO_4, 2.5 μM $ZnSO_4$, 0.5 μM $CoCl_2$, 0.5 μM $NiCl_2$, 1% BME vitamins solution (Sigma, Taufkirchen, Germany, No. B6891), the pH being adjusted to 6.5 using orthophosphoric acid. Solid minimal medium contained additionally 2% (w/v) Agar (Sigma, No. A7921). Yeast transformation was performed according to Gietz et al. (1992). Transformed yeast cells were selected on minimal medium added with 50 mM K^+ (introduced as chloride salt). Complementation growth tests were performed with solid and liquid minimal medium added with 2 mM KCl, a condition not allowing growth of the noncomplemented Wagf2 strain. For the drop tests on solid medium, isolated yeast colonies were preincubated for 12 h in liquid culture containing 50 mM K^+. They were then diluted in fresh culture medium (final absorption at 600 nm of $\sim$0.25) and grown again until the absorption at 600 nm reached 0.6. The cells were collected, washed twice with sterile water, and resuspended in water (the absorption at 600 nm being adjusted to the desired value; see the figure legends).

Yeast two-hybrid interaction tests

The two-hybrid technique was used to identify domains responsible for the assembly of SKOR. Constructs specified in the figures were cloned into the pLexPD vector (van der Ven et al., 2000) in fusion with the LexA DNA-binding domain, and into the pAD-GAL4 vector (Stratagene, Amsterdam, The Netherlands) in fusion with the GAL4 activator domain. Combinations of these constructs were used to cotransform the L40 yeast strain, which has two independent reporter genes, *lacZ* and *HIS3*, under the control of the minimal GAL1 promoter fused to multimerized LexA binding sites. Double transformants were tested for both, growth in the absence of histidine in the medium and for β-galactosidase activity. β-galactosidase activity in liquid culture was determined using ONPG (o-nitrophenyl β-D-galactopyranoside;

Sigma, No. N1127) as substrate according to the Yeast Protocol Handbook (www.clontech.com).

In vivo radioactive protein labeling

Six injected oocytes per construct were kept in 990 μl ND96 (96 mM NaCl, 2 mM KCl, 1 mM $CaCl_2$, 1 mM $MgCl_2$, 10 mM HEPES/NaOH pH 7.4) added with 10 μl of Met-[^{35}S]-label ([^{35}S]-L-methionine, [^{35}S]-L-cysteine, *Escherichia coli* ^{35}S hydrolysate; Hartmann Analytic, Braunschweig, Germany). Oocytes were incubated for 3 days at 18°C. To isolate protein, oocytes were chilled on ice for 10 min, washed twice with ND96, and homogenized in 1 ml 10 mM K-phosphate, pH 7.4, 5 mM EDTA, 5 mM EGTA, 1 mM AEBSF, 2 μg/ml leupeptin, and 1 μg/ml aprotinin. The suspensions were centrifuged for 5 min at 100 $\times$ g. The supernatant was collected and centrifuged again for 30 min at 16,000 $\times$ g. After a washing step with the homogenization medium, the pellet was resuspended in 60 μl gel loading buffer, and incubated for 6 min at 55°C. The amount of radioactivity present in the sample was determined with a liquid scintillation (LS) counter (Beckman Coulter LS6500, Unterschleissheim, Germany). Aliquots corresponding to 10^5 cpm were loaded onto 10% SDS-PAGE gels. After electrophoresis, the gels were dried and exposed to x-ray films overnight at room temperature.

Protein expression in tobacco BY2 protoplasts and targeting of GFP-fusion constructs

Suspension cultures of tobacco BY2 cells (*Nicotiana tabaccum* L. cv. Bright Yellow 2) were maintained in LS medium containing 0.2 mg/l 2,4-dichlorophenoxyacetic acid (2,4-D) in the dark at 26°C. For transformation 10-day-old cultures were harvested by vacuum filtration on a nylon membrane, resuspended (1g/10 ml) in enzyme solution (0.1% pectolyase Y-23, 0.2% driselase, 1% cellulase, 25 mM MES/KOH, 0.6 M mannitol, pH 5.5), and incubated in the dark (shaker, 50 rpm; 35°C; 3 h). Protoplasts were recovered by centrifugation (1200 $\times$ g), washed with HEPES buffer (25 mM HEPES, 0.6 M sorbitol, pH 6.7) and purified by gradient centrifugation (HEPES buffer with 0%, 10%, and 20% Ficoll, 30 min. at 1200 $\times$ g). Protoplasts collected from the interfaces were washed twice with W5 solution (154 mM NaCl, 125 mM $CaCl_2$, 5 mM KCl, 5 mM glucose, 100 mM mannitol, 0.1% MES, pH 5.8) and resuspended to a concentration of 3 $\times$ 10^6 cells/ml in MaMg solution (0.55 M mannitol, 15 mM $MgCl_2$, 0.1% MES, pH 5.8). For the transformation ($\sim$1 $\times$ 10^6 cells per transformation) a heat shock of 45°C was applied for 5 min followed by the immediate cooling on ice for 5 min. Subsequently, the plasmid DNA (containing the coding region of the fusion protein under the control of the CaMV 35S Promoter, 30 μg) and 50 μg of carrier herring sperm DNA were added. After 5-min incubation at room temperature an equal volume of PEG solution (0.1 M $Ca(NO_3)_2$, 0.5 M mannitol, 0.1% MES, pH 6.5, 40% PEG 3350) was added. After an additional 20 min at room temperature the transformation mix was supplemented with 4 ml of culture medium (LS medium + 0.4 M mannitol) and transferred to small Petri dishes. These were incubated at 26°C without shaking in the dark for 2 days. For the analysis of GFP fluorescence, protoplasts were collected by centrifugation (1200 $\times$ g, 5 min) and resuspended in 1.5 ml W5 solution. GFP fluorescence was analyzed by confocal laser scanning microscopy (Leica DM IRBE inverse microscope with Leica TCS SP laser scanning unit).

Mathematical description of yeast growth rate under limiting conditions

Yeast growth was described as follows. Yeast cells, number n, proliferate with a rate $dn/dt = \beta \times n(t) \times r(t)$. Under optimal conditions, i.e., in an infinite volume of liquid culture and with a constant level of ''resources'' needed for growth, e.g., a high concentration of K^+, the resource function $r(t)$ would be set to the constant value of 1. Cells would proliferate with the rate $\beta \times n(t)$ resulting in exponential growth. Under experimental conditions, however, i.e., in a finite volume and with consumption of resources (K^+), the resource function decreases below 1 with cell proliferation. The decrease is defined proportional to the increase in cell number as $dr = -\gamma \times dn$. At the saturation level the resource function is $r(t \rightarrow \infty) = 0$ and therefore $dn/dt = 0$, and $n(t \rightarrow \infty) = n_\infty$. Because the cell number is proportional to the optical density measured at $\lambda = 600$ nm, the n values can be replaced by $OD600$ values without changing the structure of the equations. An analytical solution of the two coupled differential equations is $OD600(t) = (OD_\infty \times OD_0)/[OD_0 + (OD_\infty - OD_0) \times \exp(-t/\tau)]$. OD_0 and OD_∞ denote the optical densities at $t = 0$ and infinity, respectively. The apparent proliferation time constant, τ, is a function of the constants β and γ.

RESULTS

SKOR assembles with GORK but not with KAT1

On the basis of K_{in} and K_{weak} channels it has been proven that *Shaker*-like plant K^+ channel α-subunits can form heteromeric channels (Dreyer et al., 1997; Baizabal-Aguirre et al., 1999; Ache et al., 2001; Pilot et al., 2001; Zimmermann et al., 2001). In this study, a first set of experiments was performed to address the question of whether plant K_{out} channel subunits also contribute to the formation of heteromeric channels. After coexpression of the K_{in} channel α-subunit KAT1 and the K_{out} channel α-subunit SKOR in *Xenopus* oocytes, inward currents activating more negative than -80 mV were observed along with outward currents activating more positive than -20 mV (Fig. 1 *A*). From the analyses of the steady-state current-voltage characteristics, the simplest hypothesis was that the two current components originated from two distinct homomeric entities comprising either KAT1 or SKOR subunits (Fig. 1 *B*; cf. Ache et al., 2000, for KAT1 and GORK expressing oocytes). This interpretation was fully confirmed by coexpressing KAT1 with a dominant-negative mutant of SKOR, dnSKOR (= SKOR-G292R-D293N-A296V). When this mutant was coexpressed with the SKOR wild-type, outward-rectifying K^+ currents were efficiently suppressed. When coexpressed with KAT1, dnSKOR did not affect the current amplitude compared to the control experiment (KAT1/H_2O control: same volume of *KAT1* cRNA and same volume of water injected; not shown). In contrast, the two *Arabidopsis* K_{out} channel α-subunits SKOR and GORK were able to form heteromeric channels. When SKOR was coexpressed with a dominant-negative mutant of GORK, dnGORK (= GORK-G273R-Y274R; Hosy et al., 2003), the level of functional channels, reflected by the observed current amplitude, was significantly reduced compared to the control (SKOR/H_2O; Student's t-test, $P < 10^{-7}$). Similar findings were obtained by testing the combinations SKOR/dnSKOR, GORK/dnSKOR, and GORK/dnGORK (Fig. 1, *C* and *D*). It should be emphasized that the same amount of wild-type *SKOR*-cRNA and *GORK*-cRNA, respectively, was injected in all the oocytes, and that compared experiments were carried out at the same time interval after injection.

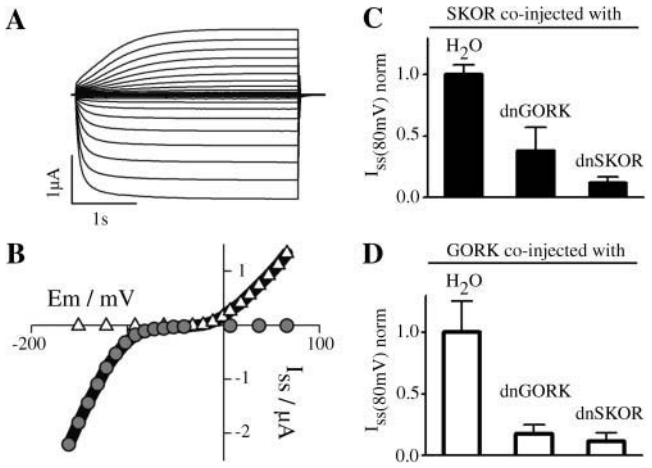

FIGURE 1 SKOR assembles with plant K_{out} but not with plant K_{in} channel α-subunits after coexpression in *Xenopus* oocytes. (*A*) Representative inward and outward K^+ currents obtained from oocytes injected with a *SKOR*/*KAT1* cRNA mixture (1:1 ratio). From a holding potential of −100 mV currents were evoked by 3.5-s activating voltage pulses from −160 mV to +70 mV (10-mV steps). (*B*) Steady-state current-voltage characteristic (*solid line*) for the oocyte shown in *A*, superimposed with the respective current-voltage relationship for homomeric KAT1 (*shaded circles*) and SKOR (*open triangles*). (*C* and *D*) Steady-state K^+ current amplitudes after coexpression (1/1 cRNA mixtures) of SKOR (*C*) and GORK (*D*) with dominant-negative mutants of SKOR (dnSKOR = SKOR-G292R-D293N-A296V) and GORK (dnGORK = GORK-G273R-Y274R). Current amplitudes were measured at the end of 3-s voltage pulses to +80 mV. To compare results obtained from different oocyte batches, the data were normalized to the mean value (I_{ss}) of the respective controls SKOR/H_2O and GORK/H_2O. Data are shown as means ± SD (n = 6–17, two different oocyte batches).

Furthermore, coexpression of a dominant-negative mutant of KAT1 (KAT1-G262R-Y263R) with SKOR and GORK affected neither the current amplitude of SKOR nor that of GORK (not shown). Therefore it could be excluded that reduced current amplitudes in coexpression experiments involving SKOR/dnSKOR, GORK/dnGORK, SKOR/dnGORK, and GORK/dnSKOR resulted from a saturation of the translation machinery of the oocyte due to an increased amount of injected cRNA. Thus, the above data clearly demonstrated that K_{out} channel α-subunits encoded by different genes form heteromeric K_{out} channels, whereas they do not coassemble with the K_{in} channel subunit KAT1.

The cytoplasmic C-terminal part of SKOR comprises the assembly domain

The region responsible for assembly of SKOR channels was narrowed down by coexpressing the entire SKOR α-subunit with N- and C-terminal truncations of itself (Fig. 2 *A*). The C-terminal deletion, SKOR-ΔCt, corresponds to the SKOR polypeptide extending from the N-terminus to the fourth transmembrane segment (S4), whereas the N-terminal deletion, SKOR-ΔNt, represents the SKOR polypeptide spanning from the fourth transmembrane region to the C-terminus. The two truncated α-subunits had different effects on the functional expression of SKOR channels. The amplitudes of the K^+ currents measured in oocytes injected with mixtures of *SKOR*/H_2O (Fig. 2 *A*, *left traces*) and *SKOR*/*SKOR*-Δ*Ct* (Fig. 2 *A*, *middle traces*) did not differ markedly from each other. The steady-state current amplitudes at +40 mV were $I_{40mV} = 1.76 \pm 0.12$ μA and 1.58 ± 0.19 μA, respectively (Fig. 2 *B*). In contrast, in oocytes injected with *SKOR*/*SKOR*-Δ*Nt* the formation of functional channels was reduced to ~20% (Fig. 2, *A* (*right traces*) and *B*). Oocytes expressing SKOR-ΔNt, SKOR-ΔCt, or SKOR-ΔNt/SKOR-ΔCt did not display any currents significantly different from the baseline in control oocytes injected with water only (not shown). Collectively, these results suggested that the assembly domain of SKOR is located in the channel region downstream of S4. Hence, the formation of functional tetrameric structures in the case of plant K_{out} channels appears not to involve an assembly domain at the N-terminus, which contrasts with the situation known from animal *Shaker* channels. Instead, assembly of plant K_{out} channels appears to be triggered via a domain(s) located at the C-terminus, like in plant K_{in} channels or animal EAG channels. To test this hypothesis further, the C-terminal part of KAT1, which is supposed to comprise the assembly domain of the channel (Marten and Hoshi, 1997), was replaced by the C-terminus of SKOR. Unfortunately, the chimera KAT1-Ct_{SKOR} appeared to be nonfunctional in oocytes: under different experimental conditions (different bath pH and K^+ concentrations), no currents different from the baseline could be elicited in the voltage interval from −170 mV to +80 mV (not shown). On the other hand, the chimera complemented the Wagf2 (Δ*trk1,2*) yeast strain (Ros et al., 1999), which is deficient in potassium uptake (Fig. 2, *C* (*left bottom*) and *D* (*open circles*)). This yeast strain, which does not display significant growth on media containing <5 mM K^+, is auxotroph for two selection markers, histidine and uracil, enabling coexpression experiments. Taking advantage of these properties in a subsequent set of experiments, the cDNAs encoding two channel α-subunits, namely KAT1 and the KAT1-Ct_{SKOR} chimera, were cloned into the low-copy (centromeric) plasmid pFL38His-PGK containing the *HIS3* marker, and those of three potential effectors, dnSKOR, SKOR-ΔCt, and SKOR-ΔNt, were cloned into the multicopy plasmid pFL61 carrying *URA3* as a marker. Yeast cells were cotransformed with pairwise combinations of these constructs and the empty vectors, and selected for the simultaneous presence of the two marker genes on K^+-rich (50 mM) medium. Positive colonies were subsequently tested for their ability to grow in low K^+ (2 mM) medium. Independent of the absence or presence of dnSKOR, SKOR-ΔCt, and SKOR-ΔNt, the empty pFL38His-PGK plasmid did not allow the mutant yeast to grow in this medium (Fig. 2, *C* (*top*) and *D* (*dashed-dotted line*)). The positive control experiment showed that yeast growth supported by KAT1 was not affected by any of

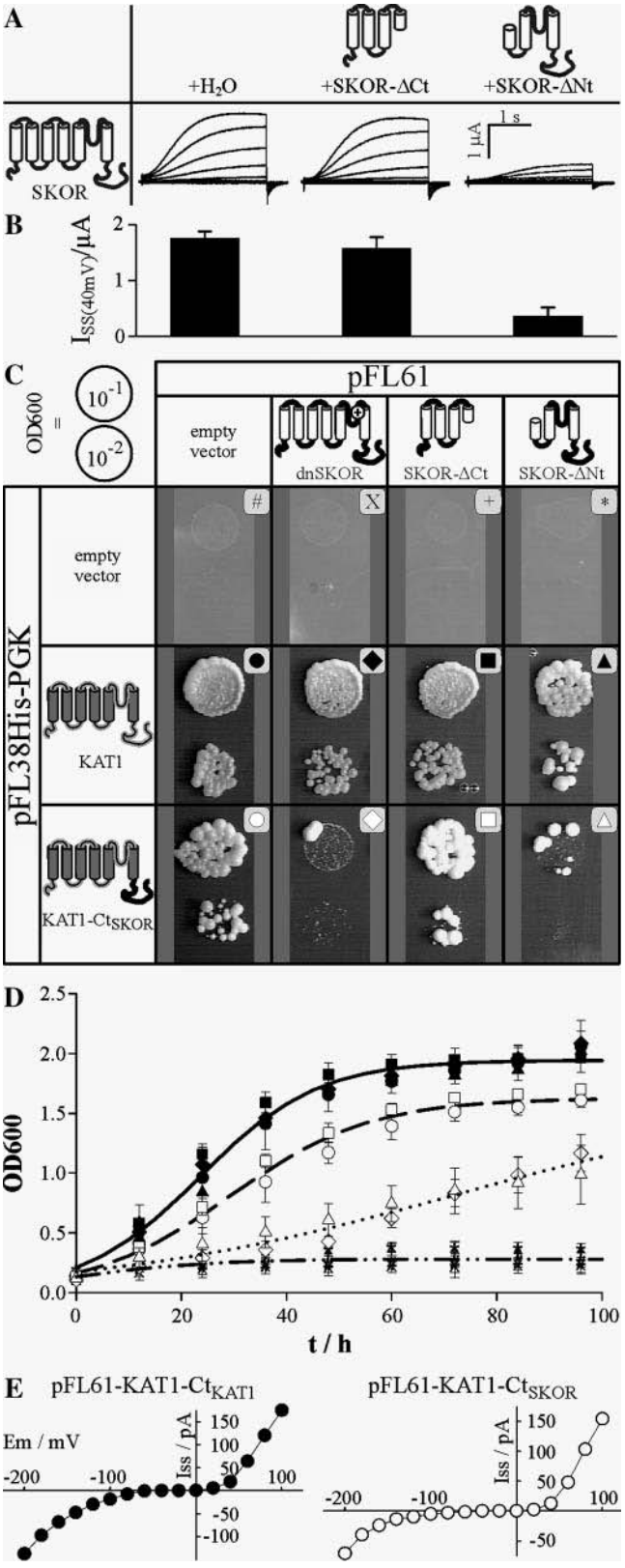

FIGURE 2 The assembly domain of SKOR is located in the cytoplasmic C-terminal part. (*A* and *B*) Coexpression of SKOR with N-terminally (SKOR-ΔNt = SKOR-M1_D172del-I173M-I174V, nomenclature according to den Dunnen and Antonarakis, 2001) and C-terminally (SKOR-ΔCt = SKOR-I211X-N212_T828del; X, stop codon) truncated SKOR proteins in *Xenopus* oocytes. (*A*) Representative K^+ currents obtained from oocytes injected with *SKOR*/*SKOR-ΔNt* (*right traces*), *SKOR*/*SKOR-ΔCt* (*middle traces*), and *SKOR*/H_2O (*left traces*) cRNA (1:1) mixtures. From a holding potential of −100 mV currents were evoked by 3-s activating voltage pulses from −120 mV to +60 mV (20-mV steps). (*B*) Mean ± SD of current amplitudes (I_{SS}) measured at the end of 3-s voltage pulses to +40 mV (n = 5–13). The data correspond to the tested combinations shown in panel *A*. (*C* and *D*) Coexpression of KAT1 and the chimera KAT1-Ct_{SKOR} (= KAT1-M1_R305-SKOR-T333_T828) with the N- and C-terminally truncated SKOR proteins SKOR-ΔNt and SKOR-ΔCt, and the dominant-negative mutant dnSKOR in the K^+ uptake deficient yeast strain Wagf2. (*C*) Drop test on solid medium. Isolated yeast colonies were preincubated overnight in liquid culture containing 50 mM K^+. After two washing steps the optical density of the cell suspension at 600 nm was adjusted to 0.1 and 0.01, respectively. These suspensions (10 µl) were dropped on plates containing 2 mM K^+ ($OD600 = 0.1$, *upper spot* in each part of the figure; $OD600 = 0.01$, *lower spot*). Plates were incubated for 5 days at 30°C. (*D*) Growth test in liquid medium. Liquid minimal medium containing 2 mM K^+ was inoculated with different yeast transformants pretreated as described in *C* so that the optical density was ~0.15. Cultures were incubated at 30°C on a shaker (190 rpm). At the time points indicated the OD600 was determined. For an explanation of the symbols, see panel *C*. Lines represent best fits with the equation $OD600(t) = (OD_\infty \times OD_0)/[OD_0 + (OD_\infty - OD_0) \times \exp(-t/\tau)]$ describing growth under limited conditions. Here, OD_0 and OD_∞ denote the optical densities at $t = 0$ and infinity, respectively. The apparent proliferation time constant is τ. Because the 12 data sets cluster into four groups, within which they do not differ significantly from each other, only one representative fit is displayed for each group. One group comprises the data obtained with KAT1 as target (*solid symbols*, *solid line*): $OD_0 = 0.21$, $OD_\infty = 1.94$, $\tau = 11.2$ h. A second group includes the control data from the empty pFL38H-PGK vector (#, X, +, *, *dashed-dotted line*): $OD_0 = 0.20$, $OD_\infty = 0.28$. A third group contains the data obtained with the chimera KAT1-Ct_{SKOR} alone and in coexpression with SKOR-ΔCt (*open circles* and *open squares*, *dashed line*): $OD_0 = 0.16$, $OD_\infty = 1.62$, $\tau = 13.4$ h. The fourth group consists of data gained with the chimera KAT1-Ct_{SKOR} as target in coexpression with dnSKOR and SKOR-ΔNt (*open diamonds* and *open triangles*, *dotted line*): $OD_0 = 0.17$, $OD_\infty = 1.64$, $\tau = 33.9$ h. The data represent the means ± SD of three to four independent samples. (*E*) Representative steady-state current-voltage characteristics obtained from patch-clamped Wagf2 yeast cells expressing a pFL61-KAT1-Ct_{KAT1} construct (*left*) and a pFL61-KAT1-Ct_{SKOR} construct (*right*). Note that outward currents at positive potentials are flowing through the depolarization-activated endogenous TOK1 channel. Data are representative for four repeats.

the SKOR-based constructs (Fig. 2, *C* (*middle*) and *D* (*solid symbols*)). This observation confirmed the result obtained in oocytes, where KAT1 did not functionally interact with SKOR. In contrast, yeast growth mediated by the chimera KAT1-Ct_{SKOR} (Fig. 2 *C*, *bottom*) was selectively inhibited by dnSKOR and SKOR-ΔNt (Fig. 2 *D*, *open diamonds* and *open triangles*), whereas the presence of SKOR-ΔCt had no inhibiting effect (Fig. 2 *D*, *open squares*). By fitting the time course of yeast growth with a mathematical function that describes growth under limiting nutrient (K^+) conditions (Fig. 2 *D*, *lines*), we were able to quantify and interpret the differences between the distinct genotypes in the following way. The growth of KAT1 expressing cells saturated at an optical density of $OD_\infty = 1.9$, whereas growth of the cells expressing KAT1-Ct_{SKOR} did at $OD_\infty = 1.6$, indicating a less

efficient exploitation of the limiting K^+ resource by the chimera in comparison with the wild-type KAT1. Additionally, yeast cells coexpressing KAT1-Ct_{SKOR} and dnSKOR, or SKOR-ΔNt, showed a τ-value 2.5 times larger than the control (KAT1-Ct_{SKOR}/empty pFL61). This is equivalent to a 40% reduction in the proliferation rate constant β (see Materials and Methods), likely to be the consequence of a reduced potassium uptake rate in these cells. The whole set of data therefore indicated that the chimera KAT1-Ct_{SKOR}, by interacting with dnSKOR and SKOR-ΔNt in yeast, exhibited the same behavior as SKOR in *Xenopus* oocytes. Thus, KAT1-Ct_{SKOR} combined characteristic functional features of the parental channels KAT1 and SKOR: from KAT1 it inherited the ability to complement a potassium uptake-deficient yeast strain, and from SKOR it inherited its assembly domain located at the C-terminus. This conclusion was further substantiated by electrophysiological studies of yeast cells transformed with a pFL61-KAT1-Ct_{SKOR} construct. Patch-clamp analyses and comparisons with yeast cells transformed with a pFL61-KAT1-Ct_{KAT1} construct indicated that this chimera mediated potassium inward currents (Fig. 2 *E*).

The role of the putative cyclic-nucleotide binding domain in SKOR channel assembly

To gain further clues on the molecular basis of SKOR channel assembly, its cytoplasmic C-terminus was analyzed for the presence of functional domains. Sequence comparisons with motifs in protein databases and in other plant K^+ channels identified three domains (Fig. 3 *A*). The region from L419 to H511 shows high homology (40% identity) to the motif pfam00027 (http://www.sanger.ac.uk/Software/Pfam/index.shtml) representing a cyclic-nucleotide binding domain (cNBD). The region from D580 to R709 contains six ankyrin motif repeats (forming the so-called ankyrin domain; Sentenac et al., 1992; Gaymard et al., 1998). The region from G774 to T828 (K_{HA}) is rich in acidic amino acid residues similar to the K_{HA}-domain previously characterized in the potato K_{in} channel KST1 (Ehrhardt et al., 1997). To uncover the role of the different domains, deletions in both, the SKOR wild-type polypeptide and the dominant-negative mutant dnSKOR were generated. The deleted polypeptide SKOR-ΔcNBD (= SKOR-D438_L506del; nomenclature according to den Dunnen and Antonarakis, 2001) lacks 69 amino acid residues within the putative cNBD, and SKOR-Δ746 (= SKOR-K746X-E747_T828del; X, stop codon) lacks the last 83 residues of the polypeptide including the K_{HA} domain (last 55 amino acids). After expression in oocytes, SKOR-Δ746 mediated potassium currents reminiscent of the wild-type SKOR channel (not specifically illustrated, but see Fig. 3 *B*, *shaded columns*), whereas SKOR-ΔcNBD remained electrically silent (not shown). In coexpression experiments only dnSKOR-Δ746 was found to affect the expression level of functional SKOR channels

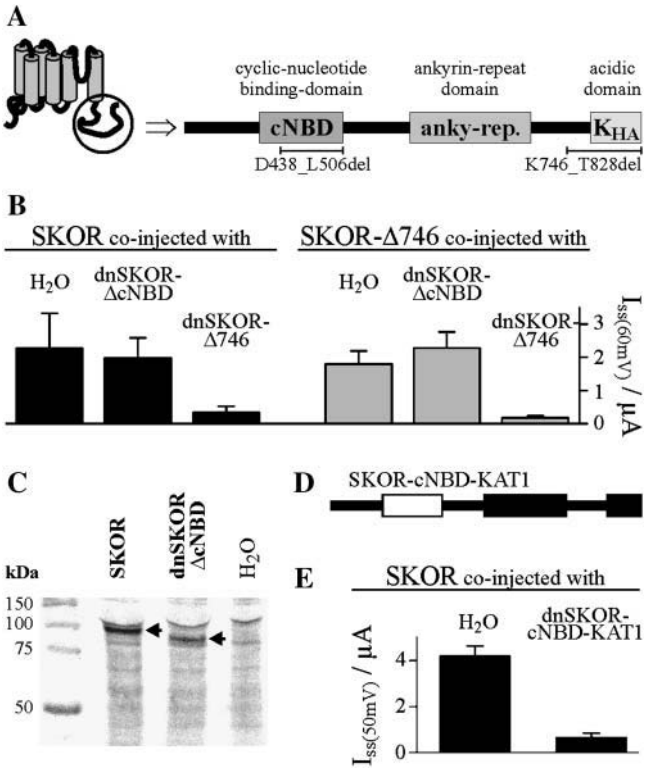

FIGURE 3 The putative cyclic-nucleotide binding domain, but not the acidic domain, is essential for SKOR assembly. (*A*) Schematic representation of the cytoplasmic SKOR C-terminus. The C-terminus contains three regions showing strong homology to previously characterized functional domains: a cyclic-nucleotide binding domain (*cNBD*), an ankyrin domain (*anky-rep.*), and an acidic domain (K_{HA}). (*B*) K^+ current amplitudes (I_{SS}) measured in oocytes after coexpression (injection of 1:1 cRNA mixtures) of SKOR (*solid columns*) and SKOR-Δ746 (= SKOR-K746X-E747_T828del, *shaded columns*), respectively, with dominant-negative mutants of SKOR-Δ746 (dnSKOR-Δ746 = SKOR-G292R-D293N-A296V-K746X-E747_T828del, *right columns*) and SKOR-ΔcNBD (dnSKOR-ΔcNBD = SKOR-G292R-D293N-A296V-D438_L506del, *middle columns*), and H_2O (*left columns*). Current amplitudes were measured at the end of 3-s voltage pulses to +60 mV. Data are shown as means ± SD (n = 3–6). (*C*) The protein dnSKOR-ΔcNBD is expressed in *Xenopus* oocytes. ^{35}S-labeled proteins obtained from water-injected control oocytes (*right lane*) and oocytes injected with *SKOR* or *dnSKOR-ΔcNBD* cRNA, respectively (*left* and *middle lanes*). Proteins were analyzed by SDS-PAGE followed by autoradiography. Molecular weight markers are on the left. Calculated molecular weights are 93.9 kDa for SKOR, and 86.1 kDa for dnSKOR-ΔcNBD. Arrows indicate the heterologously expressed proteins. (*D*) C-terminus of the chimera dnSKOR-cNBD-KAT1. The cNBD of SKOR (fragment SKOR-E410_L530) was replaced by the cNBD of KAT1 (fragment KAT1-N384_L493, *white rectangle*). (*E*) K^+ current amplitudes (I_{SS}) measured in oocytes after coexpression (injection of 1:1 cRNA mixtures) of SKOR with the dominant-negative mutant dnSKOR-cNBD-KAT1 (*right column*) or H_2O (*left column*). Current amplitudes were measured at the end of 3-s voltage pulses to +50 mV. Data are shown as means ± SD (n = 5–6).

(estimated from the amplitude of the exogenous currents): as shown in Fig. 3 *B* (*solid columns*), the presence of the dnSKOR-Δ746 α-subunit resulted in an ~85% decrease in current amplitude, whereas the presence of dnSKOR-

ΔcNBD did not significantly affect the current of SKOR. Similar results were obtained using SKOR-Δ746 as target α-subunit (Fig. 3 *B*, *shaded columns*). When compared with SKOR-Δ746 expressing oocytes, current amplitudes were strongly reduced in oocytes coexpressing SKOR-Δ746 and dnSKOR-Δ746. In contrast, a reduction of functionally active channels was not observed after coinjection of *SKOR-Δ746/dnSKOR-ΔcNBD* cRNA mixtures. The lack of currents in oocytes injected with *SKOR-ΔcNBD* cRNA, and the absence of any effect of dnSKOR-ΔcNBD in coexpression studies could be caused by some disruption of an essential assembly domain due to the deletion in the cNBD. Alternatively, it is possible that the protein encoded by the modified *(dn)SKOR-ΔcNBD* cRNAs or even the cRNA itself is rapidly degraded in oocytes. If this were the case, dnSKOR-ΔcNBD polypeptides would not be able to interact with SKOR α-subunits. To check for this possibility, three batches of oocytes injected with *SKOR*-cRNA, *dnSKOR-ΔcNBD*-cRNA, or H_2O, respectively, were incubated with ^{35}S-labeled methionine and cysteine. After 3 days of incubation, proteins were extracted from the oocytes, separated by SDS-PAGE, and visualized by autoradiography (Fig. 3 *C*). The lane corresponding to SKOR-injected oocytes specifically displayed a band close to the 100-kDa marker (*left lane*). The deletion of 69 amino acids in dnSKOR-ΔcNBD resulted in a band with a slightly smaller apparent molecular weight (*middle lane*). Both bands were absent from H_2O-injected control oocytes (Fig. 3 *C*, *right lane*). The position of the two polypeptide bands corresponded quite well with the theoretical calculations of 93.9 kDa and 86.1 kDa for the molecular weight of monomeric SKOR and dnSKOR-ΔcNBD, respectively. Thus, the polypeptide dnSKOR-ΔcNBD was expressed in oocytes. However, an investigation of the subcellular localization of a GFP-dnSKOR-ΔcNBD fusion protein in tobacco BY2 cells using a confocal laser scanning microscope revealed that it was not targeted to the plasmamembrane. Instead it accumulated in the ER (not shown), a result well known for mutants of animal channel proteins that exhibit a distorted or disrupted assembly behavior (Ma and Jan, 2002; Jenke et al., 2003).

To unravel the role of the cNBD in SKOR channel assembly the entire cyclic nucleotide-binding domain of the mutant dnSKOR (dnSKOR-E410_L520) was replaced by the corresponding domain of KAT1 (KAT1-N384_L493, Fig. 3 *D*). The two cNBDs are supposed to have a similar structure but share an identity of only 30% (for comparison: the cNBDs of SKOR and GORK are 70% identical). Upon coexpression with the SKOR wild type the dnSKOR-cNBD-KAT1 chimeric protein displayed a dominant-negative behavior (Fig. 3 *E*) identical to the mutant dnSKOR-cNBD-SKOR (= dnSKOR; Fig. 1 *C*). We concluded that in the deletion mutants (dn)SKOR-ΔcNBD misfolding of the polypeptide likely disrupted functional channel assembly and affected its targeting. This defect could be compensated by the presence of the KAT1-cNBD. Therefore it appears that the cNBD is essential for SKOR assembly by maintaining the structural integrity of the protein. The cNBD, itself, however, does not determine the specificity of the assembly.

Two-hybrid analyses to map physical interactions within the C-terminal region

To gain further insights into the assembly behavior of SKOR physical protein-protein interactions were tested employing the yeast two-hybrid system. In a first set of experiments, the cytoplasmic C-termini downstream of the membrane-spanning domains of SKOR and GORK were fused to the LexA DNA binding domain and to the GAL4 activator domain. After pairwise coexpression in yeast, growth on histidine-free medium and expression of β-galactosidase activity were detected in all possible combinations (Fig. 4 *A*). These results indicated that the C-terminus of SKOR, which comprises the domain(s) required for channel assembly (compare Figs. 2 and 3), does physically self-interact. The fact that identical results were obtained for both, the C-terminus of SKOR and GORK, suggests a similar assembly mechanism for the two plant K_{out} channels. Finally, the physical interaction between Ct-SKOR and Ct-GORK revealed by the two hybrid tests (Fig. 4) is very likely a major reason for the formation of heteromeric channels in *Xenopus* oocytes (Fig. 1, *C* and *D*).

In a following set of experiments, seven regions of the C-terminus of SKOR were defined and named A–G (Fig. 4 *B*). Nine deletions were generated as shown in Fig. 4 *B*. The construct ABCDEF- is identical to the C-terminus of the mutant SKOR-Δ746, and AB-DEFG to the C-terminus of dnSKOR-ΔcNBD. Unfortunately, six of the nine constructs fused to the LexA DNA binding domain in pLexPD showed autoactivity when cotransformed with the empty plasmid pAD-GAL4 and tested for growth on histidine-free medium. Two-hybrid combinations involving these six constructs were consequently not further considered for analyses of β-galactosidase activities. Twenty-five construct pairs were tested for protein-protein interactions in both reporter assays (Fig. 4 *C*). The following results were obtained: When the cNBD was deleted (AB-DEFG) no positive signal could be observed in any of the combinations tested, indicating that the presence of the cNBD, maintaining the structural integrity of the polypeptide, is essential not only for channel assembly but also for the physical interaction of the C-termini of both, SKOR and GORK. The cNBD alone apparently was not actively involved in establishing the interaction because the two-hybrid tests were negative when any one of the tested constructs was restricted to the cNBD alone (--C----), or to a region starting with this domain and ending at the channel C-terminus (--CDEFG). The fact that the constructs ABC---- and -BCDEFG interacted with Ct-SKOR (whereas --CDEFG did not), suggested that region B (representing a 33 amino acid stretch just upstream of the

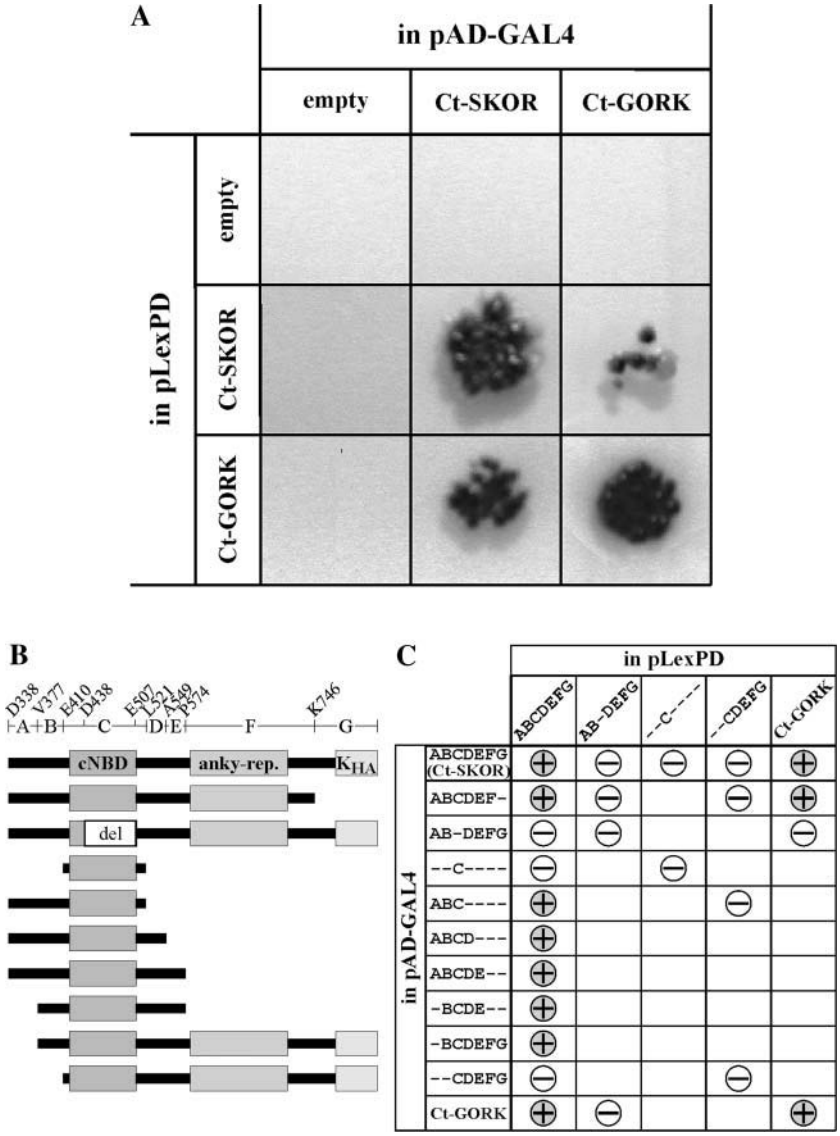

FIGURE 4 Intermolecular interaction of SKOR and GORK, and different SKOR C-terminal fragments tested in the yeast two-hybrid system. (*A*) Reciprocal interactions between SKOR and GORK C-termini. C-termini (SKOR-D338_T828, GORK-N324_T820) were fused to the LexA DNA binding domain of the vector pLexPD and to the GAL4 activator domain of the vector pAD-GAL4. Interactions were monitored in a drop test (10 μl, OD600 adjusted to 0.1) on Leu^--Trp^--His^- medium containing 5-bromo-4-chloro-3-indolyl-beta-D-galactopyranoside. Growth and blue dye formation report the physical association of the coexpressed fusion proteins. (*B*) Generation of fragments of the cytoplasmic SKOR C-terminus. The SKOR C-terminus was subdivided into seven regions (*A–G*). The position of the first amino acid of each region is indicated. Additionally, the positions D438 and E507 within region C are specified. Ten constructs were created and fused to the LexA DNA binding domain and the GAL4 activator domain, respectively. (*C*) Detection of protein associations in growth tests on Leu^--Trp^--His^- medium, and by analyzing β-galactosidase activities. A positive answer in both tests is denoted by a ''(+)'', a negative answer by a ''(−)''. Combinations indicated by empty fields have not been tested. The fragments ABCDEF-, ABC----, ABCD---, ABCDE--, -BCDE--, and -BCDEFG fused to the LexA DNA binding domain showed autoactivity (not shown). Results obtained with these constructs are not presented and are not taken into account for the interpretation of the data. The presented results are representatives of three to seven independent experiments each.

cNBD) plays an important role in triggering the physical interactions of the K_{out} channel C-termini.

Mapping C-terminal assembly domains by functional tests

To investigate which domains of the SKOR C-terminal region play a role in the formation of active channels, functional approaches were developed in both, yeast and *Xenopus* oocytes. In yeast, we tested the ability of different new chimeric constructs to complement a strain defective for K^+ uptake. These constructs were obtained by concatenating the KAT1 transmembrane channel core (KAT1-M1_R305) with C-terminal chimeras, which themselves consisted of parts of the KAT1 and SKOR C-terminal regions. Generation of the C-terminal chimeras was based on sequence comparisons of the C-terminal regions of SKOR and KAT1. Both segments display a similar structural organization except that an ankyrin domain is present in the C-terminal part of SKOR, downstream of the cNBD, but is absent from the C-terminal region of KAT1 (Figs. 4 *B* and 5 *A*). The C-termini of both channel α-subunits were subdivided into six regions. The first five parts coincided with the fragments A–E previously defined, and the sixth region corresponded to the combined fragments F and G (compare Fig. 4 *B* with Fig. 5 *A*). In all C-terminal chimeras, the region C (the cNBD) was fixed to originate from SKOR. The other regions were successively transferred from KAT1 to SKOR. In total, 12 chimeric constructs were created (Fig. 5, *A* and *B*). Each construct was defined by a stretch of six letters, either s or k, corresponding to the six successive regions from A to F/G, an s indicating that the referred region was from SKOR, and a k that the region was from KAT1. The C-terminal chimeras were fused to the hydrophobic core of KAT1 and expressed

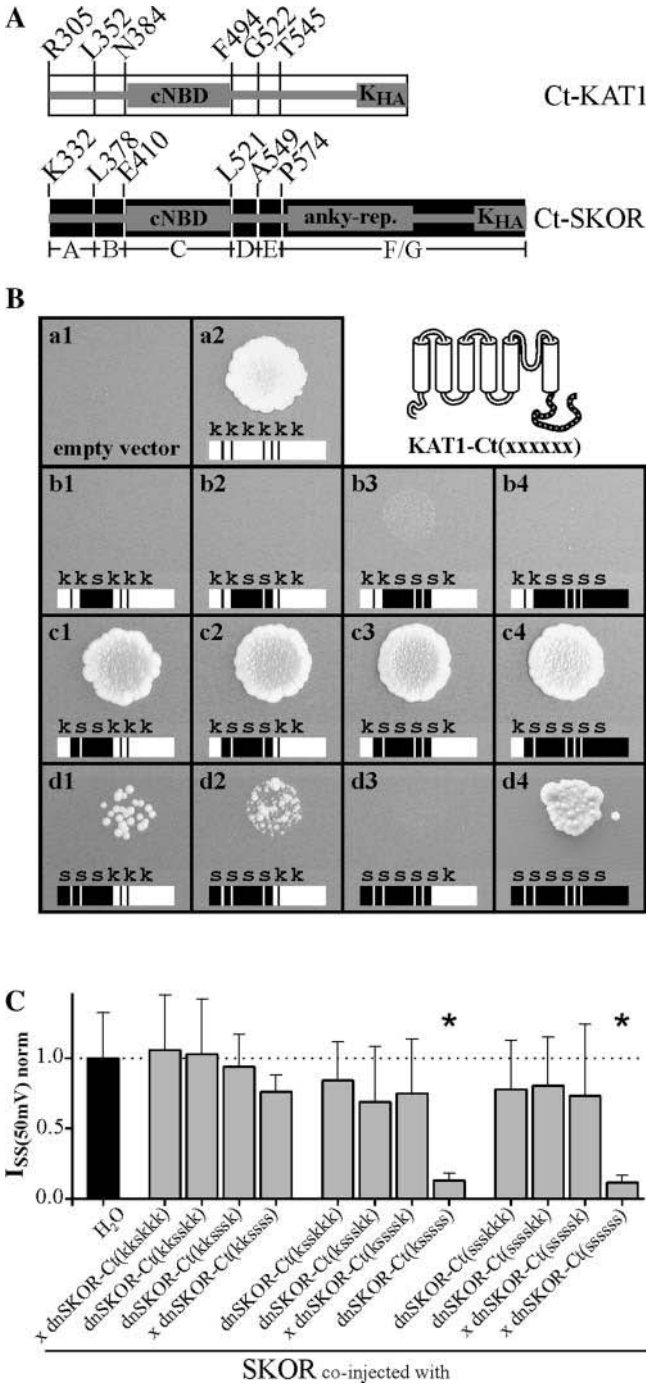

FIGURE 5 Refined SKOR/KAT1 chimeras analyzed in yeast growth tests and by coexpression with SKOR in oocytes. In the KAT1 channel several parts of the C-terminus were replaced by equivalent parts from SKOR. (*A*) The division of each C-terminus into six regions is represented schematically. The position of the first amino acid of each region is indicated. The separation (*A–G*) illustrates the division made in Fig. 4. (*B*) In the chimeras containing the KAT1 core and the chimeric C-termini, C-terminal parts originating from KAT1 are illustrated by white rectangles, and parts from SKOR by black rectangles. Additionally, the origin of the different C-terminal parts is indicated by a six-letters patch, ''xxxxxx'', where ''x'' can be ''k'' (of KAT1 origin) or ''s'' (of SKOR origin). The six white rectangles and kkkkkk (*B*, *a2*) represent the KAT1 channel, the six black rectangles and ssssss (*B*, *d4*) the chimera KAT1-Ct_{SKOR} (cf. Fig. 2 *C*).

in the yeast strain Wagf2. Positive colonies were tested for their ability to grow in low K^+ conditions. As already shown in Fig. 2 *C*, KAT1 (i.e., KAT1-Ct(kkkkkk), according to the above-defined nomenclature, Fig. 5 *B*, *a2*) as well as the chimera KAT1-Ct_{SKOR} (KAT1-Ct(ssssss), Fig. 5 *B*, *d4*) complemented the mutant yeast strain. When region C (i.e., cNBD) in KAT1 was replaced by the corresponding region of SKOR, the construct (i.e., the kkskkk chimera) was found to no longer complement the yeast cells (Fig. 5 *B*, *b1*). Further k-to-s substitutions toward the C-terminus (chimeras kksskk, kksssk, and kkssss) did not restore the ability of the chimeric proteins to complement the yeast mutant. Importantly, however, this ability was restored by introducing k-to-s substitutions toward the N-terminus: When the second region (region B) was of SKOR origin, the resulting chimeras (ksskkk, kssskk, kssssk, and ksssss) appeared to be as efficient in complementing the yeast mutant cells (Fig. 5 *B*, *c1*, *c2*, *c3*, and *c4*) as the wild-type KAT1 control. Finally, substituting the KAT1-derived A region for the corresponding region of SKOR origin gave surprising results: the resulting chimeras were less efficient (chimeras sssskk and sssssk; Fig. 5 *B*, *d1* and *d2*) or not at all able (chimera ssssssk, Fig. 5 *B*, *d3*) in complementing the yeast mutant.

Taken together, the yeast complementation experiments revealed that at least seven of the twelve chimeric α-subunits were able to assemble into functional channels. In all functional chimeric proteins fragments B and C were of SKOR origin, indicating a dominant role of the region located upstream of the cNBD not only for physical C-terminal interactions, but also for the formation of functional channels.

Evidence for a further site involved in SKOR channel formation

The yeast experiments above provided some useful but still incomplete information: On the one hand, the functionality of a chimera indicates that its assembly mechanism is intact.

Only chimeras containing the cNBD from SKOR (xxsxxx) were tested. Note that the C-terminus of KAT1 is shorter than that of SKOR because it does not contain an ankyrin domain. The chimeras were expressed in the potassium uptake deficient yeast strain Wagf2 and analyzed in drop tests (10 μl, OD600 adjusted to 0.1) on minimal medium supplemented with 2 mM K^+. The presented results are representative for at least three repeats. (*C*) Coexpression (1:1 cRNA mixtures) of SKOR with chimeric mutants in *Xenopus* oocytes. The chimeric mutants are built of the core (Nterm-S6) of dnSKOR (= SKOR-G292R-D293N-A296V) and the chimeric C-termini as displayed in panel *B*. Current amplitudes (I_{SS}) were measured at the end of 2-s voltage pulses to +50 mV. To compare results obtained from different oocyte batches, the data were normalized to the mean value of the control SKOR/H_2O (*solid column*). Data are shown as means ± SD ($n = 5$–18, six different oocyte batches). The asterisks indicate combinations where the mutant showed a strong dominant-negative effect, i.e., ≈80% reduction in the K^+ current amplitude (Student's *t*-test, $P < 10^{-7}$). The expression of five constructs (marked with *x*) was verified in ^{35}S-protein-labeling experiments.

However, the assembly mechanism of a functional chimera is not necessarily identical to that of SKOR. On the other hand, the lack of demonstration of function for a chimera is not automatically an indication for a distorted assembly mechanism. Therefore, the C-terminal chimeras, tested in the preceding experiment, were fused to the hydrophobic core of the dominant-negative mutant channel dnSKOR. The resulting constructs were coexpressed with the wild-type SKOR channel in *Xenopus* oocytes. Using ^{35}S-labeled methionine and cysteine, chimerical protein expression was checked exemplarily for the constructs dnSKOR-Ct(kkskkk), dnSKOR-Ct(kkssss), dnSKOR-Ct(kssssk), dnSKOR-Ct(sssssk), and dnSKOR-Ct(ssssss) (marked *x* in Fig. 5 *C*, cf. Fig. 3 *C*). Nevertheless, coexpression of SKOR with chimeras in which region B was of KAT1 origin, i.e., chimeras of the type dnSKOR-Ct(kksxxx) (cf. Fig. 5 *B*, *b1–b4*), did not significantly influence the measured K^+ currents in comparison to SKOR/H_2O (Fig. 5 *C*). This result supported the above-made conclusion that region B (together with the cNBD, region C) plays an essential role in SKOR channel formation. Whereas region C appeared to be essential for assembly by maintaining the structural integrity of the protein, region B seemed to be involved in determining the specificity of the assembly. Interestingly, however, some chimeras in which both regions, B and C, were of SKOR origin were also not able to strongly reduce SKOR currents. Only two constructs with F/G segments of SKOR origin, i.e., the dnSKOR-Ct(kksssss) chimera and the SKOR dominant-negative mutant itself (''dnSKOR-Ct(ssssss) chimera''), were endowed with a strong dominant-negative behavior (Fig. 5 *C*). These data suggested the presence of another domain in the far C-terminus (in region F/G) involved in the formation of tetrameric channels. This hypothesis was also supported by the fact that the functional chimeras KAT1-Ct(ssskkk), KAT1-Ct(sssskk), and KAT1-Ct(ssssss) (Fig. 5 *B*, *d1*, *d2*, and *d4*) lost their ability to complement yeast when the last three segments of the constructs were deleted (resulting in the chimeric polypeptide KAT1-Ct(sss---); data not shown).

A K_T-like domain involved in SKOR channel assembly

To further analyze the role of the F/G region in channel assembly, additional chimeras, and deletions at the very C-terminus were generated in the dnSKOR mutant background (Fig. 6 *A*). When the K_{HA} domain of dnSKOR (G774_T828) was replaced by the K_{HA} domain of KAT1 (G624_N677; Fig. 6 *A*, *i*) the resulting channel exhibited dominant-negative behavior upon coexpression with wild-type SKOR (Fig. 6 *B*, *i*). However, when a slightly larger region was exchanged (KAT1-R608_N677 replacing SKOR-V752_T828; Fig. 6 *A*, *ii*), dominant-negative behavior was no longer observed. In coexpression experiments with

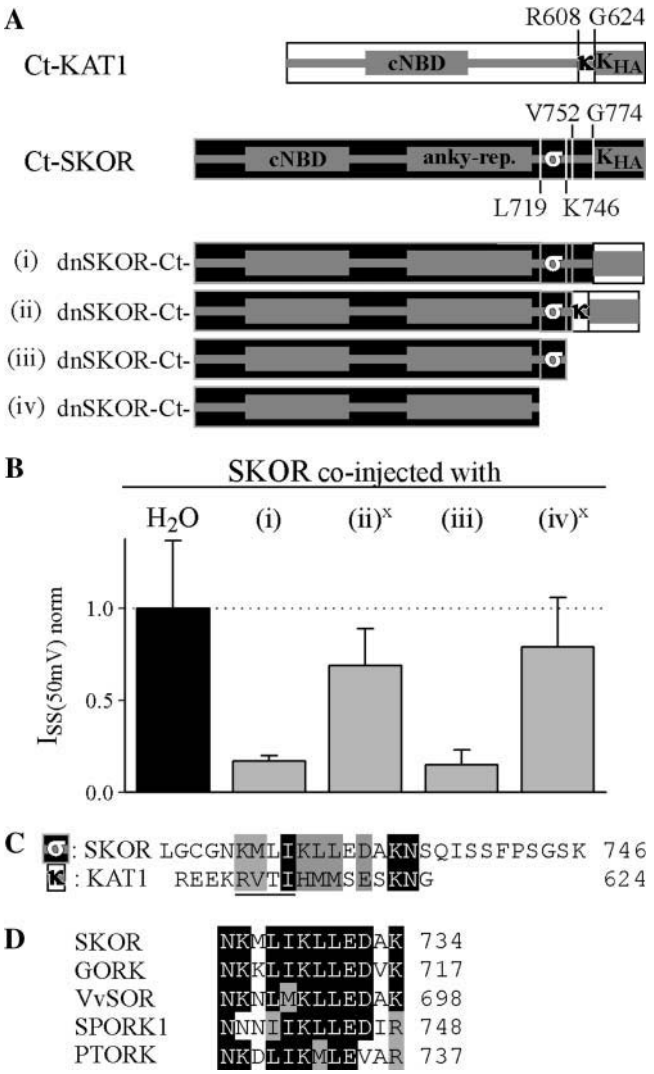

FIGURE 6 A second domain at the C-terminus is involved in SKOR channel assembly. (*A*) Generation of chimeric/truncation mutants on the basis of dnSKOR. In dnSKOR, regions at the end of the C-terminus were either deleted or replaced by equivalent parts of KAT1. The individual C-termini are represented schematically (*i–iv*). The position of the first amino acid of each region is indicated. Parts originating from KAT1 are illustrated by white rectangles, and parts from SKOR are shown as black rectangles. (*B*) Coexpression experiments (1:1 cRNA mixtures) with SKOR and the constructs shown in panel *A* in *Xenopus* oocytes. Current amplitudes (I_{SS}) were measured at the end of 2-s voltage pulses to +50 mV. To compare results obtained from different oocyte batches, the data were normalized to the mean value of the control SKOR/H_2O (*solid column*). Data are shown as means ± SD ($n = 6–12$, two different oocyte batches). The expression of the constructs (*ii*) and (*iv*) (marked with *x*) was verified in ^{35}S-protein-labeling experiments. (*C*) Sequence comparison of the regions ''σ'' (SKOR-L719_K746) and ''κ'' (KAT1-R608_G624) marked in *A*. The conserved tetra-peptide of the K_T domain ([R-V-T-I] in KAT1) is underlined. (*D*) Sequence comparison of the ''σ'' domains of the plant K_{out} channels SKOR (GenBank protein accession number CAA11280), GORK (CAC17380), *Vitis vinifera* VvSOR (CAD35400), *Samaea saman* SPORK1 (CAC10514), and *Populus tremula x tremuloides* PTORK (CAC05488).

SKOR, this mutant caused only a small decrease (30%) in the K^+ current level (Fig. 6 *B*, *ii*). When in this mutated chimera, the 70 residues of KAT1 origin as well as seven more residues of SKOR were deleted (Fig. 6 *A*, *iii* (= dnSKOR-Δ746)), the dominant-negative behavior was restored (Fig. 6 *B*, *iii*). As already shown (Fig. 3), the truncation of the terminal 83 amino acid residues of the SKOR α-subunit (SKOR-Δ746) affected neither the ability of the polypeptide to form functional channels nor its capacity to assemble with SKOR. However, the removal of 27 more residues (marked ''σ'' in Fig. 6 *A*) did. The deletion mutant SKOR-Δ719 (=SKOR-L719X-G720_T828del) did not mediate currents when expressed in *Xenopus* oocytes (not shown). Similarly, the mutant dnSKOR-Δ719 (Fig. 6 *A*, *iv*) only slightly (20%) reduced the K^+ current levels in coexpression experiments with the wild-type SKOR α-subunit (Fig. 6 *B*, *iv*). These results indicated that the two segments ''σ'' (SKOR-L719_K746) and ''κ'' (KAT1-R608_G624) are involved in determining the assembly specificity of the channel proteins. Sequence comparisons between the segments ''σ''and ''κ'' revealed some resemblance (17% identity, 67% similarity) in a 12 amino-acid-residue-long fragment (Fig. 6 *C*). In K_{in} channels, a previous study proposed that this domain, called K_T, is involved in heteromerization of K_{in} channel α-subunits encoded by different genes (Zimmermann et al., 2001). The characteristic feature of the K_T domain is a conserved tetrapeptide [R-(V/I)-(T/S/I)-(I/V)], which is at positions R612–I615 in KAT1 (*underlined* in Fig. 6 *C*), and which harbors a putative phosphorylation site. A similar motif, however, is absent in K_{out} channels. Instead, by comparing the sequences of five different K_{out} channels available from diverse plant species (Gaymard et al., 1998; Ache et al., 2000; Langer et al., 2002; Moshelion et al., 2002) a dodecapeptide consensus pattern [N-(K/N)-x-(I/L)-(I/M)-K-(L/M)-L-E-(D/N)-x-(K/R)] could be deduced (Fig. 6 *D*). In contrast to the K_T domain, this motif does not comprise any putative phosphorylation site.

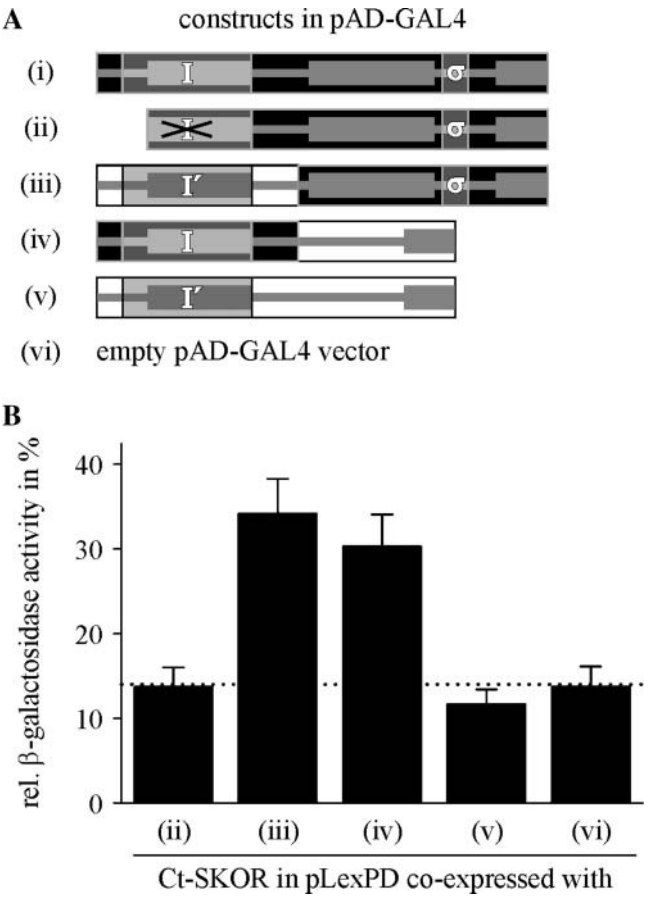

FIGURE 7 Identification of weak intermolecular interactions between Ct-SKOR and different C-terminus constructs in the yeast two-hybrid system. (*A*) Generation of chimeric/truncation mutants on the basis of the SKOR (*i*) and the KAT1 (*v*) C-terminus. The individual C-termini are represented schematically (*i–vi*). Parts originating from KAT1 are illustrated by white rectangles, and parts from SKOR are shown as black rectangles. The label ''I'' indicates the proximal interacting region of SKOR, the label ''I′'' its counterpart found in KAT1, and the label ''σ'' the distal interacting region. Note that in construct (*ii*) the proximal interacting region was partly deleted. The constructs were fused to the GAL4 activator domain. (*B*) Identification of protein interactions between Ct-SKOR (fused to the LexA binding domain) and the constructs shown in *A* by analyzing β-galactosidase activities. Data are shown as means ± SD (n = 4–8). To facilitate the comparison all values were normalized to the mean value measured for the positive control (self-interaction of Ct-SKOR = 100%, *i* in panel *A*). The dotted line indicates the background level of β-galactosidase activity measured with Ct-SKOR in combination with the empty pAD-GAL4 vector (*vi*).

The two distinct assembly regions contribute separately to the interaction of SKOR C-terminal regions

The results presented so far indicated that the specificity of SKOR channel assembly was determined by two distinct regions: segment B (Fig. 4 *B*, together with the cNBD named ''proximal interacting region'' in the following) and segment ''σ'' (Fig. 6 *A*, named ''distal interacting region'' in the following). Whereas the upstream region (labeled *I* in Fig. 7 *A*) could be correlated with direct physical interactions of the SKOR C terminus (Fig. 4), the contribution of the downstream region to channel assembly was less clear. Therefore, physical interactions of C-termini were further analyzed in yeast, using a more sensitive two-hybrid assay. Cells grown in liquid culture were tested for β-galactosidase activity using ONPG (o-nitrophenyl β-D-galactopyranoside) as substrate. The SKOR C-terminus, fused to the LexA binding domain, served as a potential target for six different constructs fused to the GAL4 DNA-binding domain (Fig. 7 *A*). When the functionality of the proximal interacting region was disrupted by deleting the essential part *B* (Fig. 7, *ii*; Fig. 4 *B* (construct --CDEFG)); reporter (β-galactosidase) activity was close to the background level (Ct-SKOR +

empty vector, Fig. 7, *vi*, and Ct-SKOR + Ct-KAT1, Fig. 7, *v*). When the proximal assembly domain was not deleted, but instead was replaced by the corresponding region of KAT1 (labeled *I′* in Fig. 7 *A*), a physical interaction with the SKOR C-terminus could be monitored (Fig. 7, *iii*). Similarly, when the downstream part of the SKOR C-terminus (comprising the distal interacting region "σ") was replaced by the distal region of the KAT1 protein, significant β-galactosidase activity was detected (Fig. 7, *iv*). Because the SKOR C-terminus did not interact with any segment of the KAT1 C-terminus (Fig. 7, *v*), these results suggested a joint contribution of the proximal and the distal assembly regions of SKOR to physical C-terminus interaction. Hereby, the contribution of the distal interacting region depends on the presence of an intact proximal assembly region.

DISCUSSION

In this report we investigated the assembly of plant *Shaker*-like K_{out} channels by combining two-hybrid assays with functional analyses, i.e., electrophysiological recordings of exogenous currents in *Xenopus* oocytes and tests of restoration of K^+ transport activity in a yeast strain deficient for K^+ uptake.

Our data demonstrate that plant K_{out} channels, like the plant K_{in} channel AKT1 (Daram et al., 1997), assemble through interaction sites located at the cytoplasmic C-terminus of the protein rather than by an N-terminal tetramerization domain. Hence, the assembly process of plant K_{out} channels, seen in the light of the present knowledge about the assembly of animal potassium channels, is more related to that of members of the EAG or KCNQ families (Ludwig et al., 1997; Schmitt et al., 2000) than to that of typical voltage-gated *Shaker* (Kv) channels (Li et al., 1992). Recent analyses revealed that channels of the EAG superfamily assemble via a tetramerizing coiled coil, a domain in which the probability for the formation of a coiled coil peaks (Jenke et al., 2003). For K_{out} and K_{in} channels, the existence of a similar domain does not seem likely. The SKOR polypeptide, for example, has been analyzed with the program Coils, Version 2.2 (Lupas et al., 1991; http://www.ch.embnet.org) to determine the local probability for coiled-coil formations. Although coiled regions were predicted with a probability of 0.77 for the section K524_I537 (fragment D in Fig. 4 *B*), and with a probability of 0.83 for the section R781_V796 (within the K_{HA} domain), the experimental data presented in this study do not provide evidence for a role of these regions in channel tetramerization. Our results rather suggest that other interaction sites drive multimerization of plant K_{out} channels: a proximal interacting region (regions B and C in Fig. 4 *B*; region I in Fig. 7 *A*), and a distal interacting region downstream of the ankyrin domain (segment "σ" in Fig. 6 *A* and in Fig. 7 *A*).

The two distinct assembly regions contribute differently to interaction of SKOR C-terminal regions

In yeast two-hybrid assays the proximal interacting region is active on its own in promoting protein-protein interactions. In contrast, the detection of interactions mediated by the distal interacting region was coupled to the presence of a functional proximal interacting region. This result may indicate that either a proximal interacting region is necessary to maintain the structural integrity of the protein, and/or that the interaction mediated by the proximal interacting region is needed as a prerequisite for the activity of the distal interacting region. In the latter case the assembly of SKOR polypeptides would involve at least two consecutive steps. In this model, the proximal interacting region would play an essential role in a first interaction process, e.g., in the dimerization of two SKOR α-subunits, causing conformational changes that then allow formerly inactive interacting regions to contribute to the subsequent steps. In other words, these newly recruited interacting sites would not belong to the α-subunit itself but to the dimer. The assembly behavior of SKOR would then be comparable to that of Kv channels that have been proposed to form tetramers from preassembled dimers (Tu and Deutsch, 1999).

Despite the apparent involvement of the distal interacting region in channel assembly it cannot, however, be excluded that it might additionally play a role in channel trafficking. Future cell-biological studies addressing channel maturation and processing will allow further conclusions in this context.

Distinct protein interactions contribute jointly to functional SKOR channel formation

It should be emphasized that the interactions identified in yeast two-hybrid experiments (Figs. 4 and 7) appeared to be contradictory to the results obtained from analyzing channel function. Positive protein-protein interaction of the construct *iv* (Fig. 7 *A*) with Ct-SKOR (Fig. 7 *B*, *iv*), for example, apparently did not fit with the negative results obtained after coexpressing dnSKOR-Ct(ssssk) and SKOR (Fig. 5 *C*). Additionally, in two-hybrid experiments Ct-SKOR was interacting with the constructs ABC----, ABCD---, ABCDE--, and -BCDE-- (Fig. 4), all of them lacking the region "σ." However, when the "σ" region was absent, no evidence for functional channel assembly could be gained in different approaches with different experimental systems: a), construct dnSKOR-Ct(sssss-) had no dominant negative effect on functional SKOR channel formation (Fig. 6 *B*, *iv*); b), the channel SKOR-Ct(sssss-) did not mediate currents (not shown); c), the chimera KAT1-Ct(sss---) did not complement yeast (not shown). These apparent discrepancies in the experimental findings may be explained by taking into account the different stringencies of the chosen assays. Whereas the low-stringent yeast two-hybrid assays

reported protein-protein interactions, the highly stringent functional assays tested for the presence of fully assembled, intact channels in the membrane. Thus, successful interaction detected in two-hybrid experiments will not necessarily translate into successful channel assembly. From the presented results we rather have to conclude that the contribution of both interacting regions, proximal and distal, is required for functional channel formation.

Assembly of SKOR in comparison to other channels

The two-hybrid tests (Fig. 4), in combination with functional assays in *Xenopus* oocytes (Fig. 1, *C* and *D*), demonstrated that the two K_{out} subunits SKOR and GORK interact and form heteromeric channels under suitable experimental conditions. Whether such interactions actually occur in planta, allowed by overlapping expression patterns of K_{out} channel genes, has to be investigated in subsequent studies. On the other hand, functional data obtained in oocytes and yeast (e.g., Fig. 1, *A* and *B*, and Fig. 2 *C*) point to the absence of heteromerization between the K_{in} channel subunit KAT1 and the K_{out} channel subunits SKOR or GORK. Nevertheless, KAT1 contains segments at its C-terminus that are functionally equivalent to the interacting regions of SKOR. In substitution experiments, the KAT1 regions compensated for the loss of the SKOR domains (Figs. 3, 5, 6, and 7). Despite these functional similarities, however, the KAT1 and SKOR regions appear not to be compatible. In yeast two-hybrid assays no interaction between the C-termini of KAT1 and SKOR could be detected. Furthermore, functional dnSKOR chimera, carrying one of the two interaction regions of KAT1, were not endowed with a strong dominant-negative behavior. Thus, the incompatibility of the C-terminal regions is very likely the molecular reason why K_{in} and K_{out} channel α-subunits do not coassemble. Additionally, the assembly of SKOR and KAT1 appeared to be different. Whereas SKOR assembles properly only in the presence of both, the proximal and the distal interacting regions (Figs. 5 and 6), KAT1 does not need a distal region for tetramerization. This channel remains functional when its complete C-terminal part downstream of the putative cyclic nucleotide-binding domain (therefore downstream of the proximal interaction region) is deleted (Marten and Hoshi, 1997). With this feature KAT1 fits well into a picture that was recently developed on the basis of the crystal structure of the C-terminus of the mouse hypolarization-activated, cyclic nucleotide-modulated channel HCN2 (Zagotta et al., 2003). In the tetrameric C-terminus of this channel a domain linking the last transmembrane segment with the cyclic nucleotide-binding domain (called ''C-linker domain,'' equivalent to the joint regions A and B in Fig. 4 *B*) mediates most of the subunit-subunit contacts. The C-linker domain consists of six α-helices, which are separated by short loops. The first two helices of each subunit (equivalent to region A in Fig. 4 *B*) form an antiparallel helix-turn-helix motif that interacts with the third and fourth helices (fourth helix is equivalent to region B in Fig. 4 *B*) of the neighboring subunit. It was suggested that KAT1-related potassium channels are related to animal HCN channels in structure and mechanism (Zagotta et al., 2003). The data available for KAT1 are in good agreement with this model. However, for SKOR the structural data of HCN2 can only partially explain the C-terminal interactions underlying channel assembly. We found that the region upstream of the cNBD has an important role in SKOR C-terminus interaction. However, this interaction is insensitive to the removal of the first 39 amino acid residues (region A; Fig. 4, *B* and *C*) that correspond to the first three interacting helices in HCN2. Furthermore, in contrast to SKOR and KAT1 (Marten and Hoshi, 1997) the assembly of HCN2 is apparently not disrupted when the cNBD is deleted. HCN2 still functions as a channel after removal of the cNBD (Wainger et al., 2001). Finally, as outlined before, subunit-subunit interactions in SKOR strongly depend on another distal region for which no equivalent part could be identified in the crystal structure of HCN2. Thus, to explain SKOR channel assembly the crystal structure data of HCN2 do not serve as a fully applicable model. However, other observations and suggestions based on the HCN2 data are very intriguing. Because the cNBD of SKOR lacks many of the key residues that were identified by Zagotta et al. (2003) in HCN2 to interact with cyclic nucleotides, it is very likely that the putative cNBD of SKOR does actually not interact with cyclic nucleotides but rather with other small (so far unknown) molecules. Future studies will clarify to what extend cyclic nucleotides modify the activity of SKOR and/or its assembly behavior.

CONCLUSION

In summary, this study provides evidence that plant K_{out} channel α-subunits, like plant K_{in} channel α-subunits, assemble via interaction domains located in the cytoplasmic C-terminal parts of the polypeptides. The data indicate that the assembly of plant K_{out} channels is a complex process involving different regions of the α-subunit: i), a proximal interacting region, consisting of two functionally distinct parts, and ii), a distal interacting region. The contribution of both regions to channel assembly appears to be different. Whereas the proximal interacting region is active on its own in promoting protein-protein interactions, the distal interacting region needs an intact proximal interacting region to be active. The contribution of both interactions is required for functional channel formation. Similar to K_{in}, K_{out} α-subunits have the potential to form heteromeric channels. However, the formation of heteromeric channels consisting of K_{in} and K_{out} α-subunits was not observed in our experiments. We rather provide evidence for the existence of barriers preventing K_{in}-K_{out} heteromerization. This result is not totally unexpected. In a physiological constellation such an

interaction would seem rather inappropriate, if not deleterious, as it would drive K^+ transport out of efficient cellular control. It appears that evolution has not only created plant K^+ channels with different rectification properties, but also mechanisms that help to avoid interactions between K_{in} and K_{out} α-subunits.

We thank Dr. Ingela Johansson, Glasgow, for the ^{35}S-labeling protocol, and Dr. Isabelle Chérel for initial help with the yeast expression system. B.M.R. thanks the Max-Planck Institute of Molecular Plant Physiology for providing lab space and electrophysiology equipment. We are grateful to two anonymous reviewers for valuable constructive criticisms that helped to improve the manuscript.

This work was partly supported by a Marie Curie Fellowship of the European Union to I.D. (contract no. ERBBIO4CT985058, proposal no. 980115), and by the GABI-Génoplante joint programs (GABI FKZ 0312852, GENOPLANTE contract no. AF2001093).

REFERENCES

Ache, P., D. Becker, R. Deeken, I. Dreyer, H. Weber, J. Fromm, and R. Hedrich. 2001. VFK1, a *Vicia faba* K^+ channel involved in phloem unloading. *Plant J.* 27:571–580.

Ache, P., D. Becker, N. Ivashikina, P. Dietrich, M. R. Roelfsema, and R. Hedrich. 2000. GORK, a delayed outward rectifier expressed in guard cells of *Arabidopsis thaliana*, is a K^+-selective, K^+-sensing ion channel. *FEBS Lett.* 486:93–98.

Ausubel, F. M., R. Brent, R. E. Kingston, D. D. Moore, J. G. Seidam, J. A. Smith, and K. Struhl. 1993. Current Protocols in Molecular Biology. Green Publishing Associates, John Wiley & Sons, New York.

Baizabal-Aguirre, V. M., S. Clemens, N. Uozumi, and J. I. Schroeder. 1999. Suppression of inward-rectifying K^+ channels KAT1 and AKT2 by dominant negative point mutations in the KAT1 alpha-subunit. *J. Membr. Biol.* 167:119–125.

Becker, D., I. Dreyer, S. Hoth, J. D. Reid, H. Busch, M. Lehnen, K. Palme, and R. Hedrich. 1996. Changes in voltage activation, Cs^+ sensitivity, and ion permeability in H5 mutants of the plant K^+ channel KAT1. *Proc. Natl. Acad. Sci. USA.* 93:8123–8128.

Bertl, A., H. Bihler, C. Kettner, and C. L. Slayman. 1998. Electrophysiology in the eukaryotic model cell Saccharomyces cerevisiae. *Pflugers Arch.* 436:999–1013.

Daram, P., S. Urbach, F. Gaymard, H. Sentenac, and I. Cherel. 1997. Tetramerization of the AKT1 plant potassium channel involves its C-terminal cytoplasmic domain. *EMBO J.* 16:3455–3463.

den Dunnen, J. T., and S. E. Antonarakis. 2001. Nomenclature for the description of human sequence variations. *Hum. Genet.* 109:121–124.

Dreyer, I., S. Antunes, T. Hoshi, B. Mueller-Roeber, K. Palme, O. Pongs, B. Reintanz, and R. Hedrich. 1997. Plant K^+ channel alpha-subunits assemble indiscriminately. *Biophys. J.* 72:2143–2150.

Dreyer, I., C. Horeau, G. Lemaillet, S. Zimmermann, D. R. Bush, A. Rodriguez-Navarro, D. P. Schachtman, E. P. Spalding, H. Sentenac, and R. F. Gaber. 1999. Identification and characterization of plant transporters using heterologous expression systems. *J. Exp. Bot.* 50:1073–1087.

Dreyer, I., B. Mueller-Roeber, and B. Köhler. 2002. New challenges in plant ion transport research: from molecules to phenomena. *In* Recent Research Developments in Molecular & Cellular Biology, Vol. 3, Part II. Research Signpost, Kerala, India. 379–95.

Ehrhardt, T., S. Zimmermann, and B. Mueller-Roeber. 1997. Association of plant K^+_{in} channels is mediated by conserved C-termini and does not affect subunit assembly. *FEBS Lett.* 409:166–170.

Gaymard, F., G. Pilot, B. Lacombe, D. Bouchez, D. Bruneau, J. Boucherez, N. Michaux-Ferriere, J. B. Thibaud, and H. Sentenac. 1998. Identification and disruption of a plant shaker-like outward channel involved in K^+ release into the xylem sap. *Cell.* 94:647–655.

Gietz, D., A. St Jean, R. A. Woods, and R. H. Schiestl. 1992. Improved method for high efficiency transformation of intact yeast cells. *Nucleic Acids Res.* 20:1425.

Hosy, E., A. Vavasseur, K. Mouline, I. Dreyer, F. Gaymard, F. Poree, J. Boucherez, A. Lebaudy, D. Bouchez, A. A. Very, T. Simonneau, J. B. Thibaud, and H. Sentenac. 2003. The *Arabidopsis* outward K^+ channel GORK is involved in regulation of stomatal movements and plant transpiration. *Proc. Natl. Acad. Sci. USA.* 100:5549–5554.

Jenke, M., A. Sanchez, F. Monje, W. Stuhmer, R. M. Weseloh, and L. A. Pardo. 2003. C-terminal domains implicated in the functional surface expression of potassium channels. *EMBO J.* 22:395–403.

Lacombe, B., and J. B. Thibaud. 1998. Evidence for a multi-ion pore behavior in the plant potassium channel KAT1. *J. Membr. Biol.* 166: 91–100.

Langer, K., P. Ache, D. Geiger, A. Stinzing, M. Arend, C. Wind, S. Regan, J. Fromm, and R. Hedrich. 2002. Poplar potassium transporters capable of controlling K^+ homeostasis and K^+-dependent xylogenesis. *Plant J.* 32:997–1009.

Li, M., Y. N. Jan, and L. Y. Jan. 1992. Specification of subunit assembly by the hydrophilic amino-terminal domain of the Shaker potassium channel. *Science.* 257:1225–1230.

Ludwig, J., D. Owen, and O. Pongs. 1997. Carboxy-terminal domain mediates assembly of the voltage-gated rat ether-a-go-go potassium channel. *EMBO J.* 16:6337–6345.

Lupas, A., M. Van Dyke, and J. Stock. 1991. Predicting coiled coils from protein sequences. *Science.* 252:1162–1164.

Ma, D., and L. Y. Jan. 2002. ER transport signals and trafficking of potassium channels and receptors. *Curr. Opin. Neurobiol.* 12:287–292.

Marten, I., and T. Hoshi. 1997. Voltage-dependent gating characteristics of the K^+ channel KAT1 depend on the N and C termini. *Proc. Natl. Acad. Sci. USA.* 94:3448–3453.

Maser, P., S. Thomine, J. I. Schroeder, J. M. Ward, K. Hirschi, H. Sze, I. N. Talke, A. Amtmann, F. J. Maathuis, D. Sanders, J. F. Harper, J. Tchieu, M. Gribskov, M. W. Persans, D. E. Salt, S. A. Kim, and M. L. Guerinot. 2001. Phylogenetic relationships within cation transporter families of *Arabidopsis*. *Plant Physiol.* 126:1646–1667.

Minet, M., M. E. Dufour, and F. Lacroute. 1992. Complementation of *Saccharomyces cerevisiae* auxotrophic mutants by Arabidopsis thaliana cDNAs. *Plant J.* 2:417–422.

Moshelion, M., D. Becker, K. Czempinski, B. Mueller-Roeber, B. Attali, R. Hedrich, and N. Moran. 2002. Diurnal and circadian regulation of putative potassium channels in a leaf moving organ. *Plant Physiol.* 128:634–642.

Pilot, G., F. Gaymard, K. Mouline, I. Cherel, and H. Sentenac. 2003a. Regulated expression of *Arabidopsis* shaker K^+ channel genes involved in K^+ uptake and distribution in the plant. *Plant Mol. Biol.* 51: 773–787.

Pilot, G., B. Lacombe, F. Gaymard, I. Cherel, J. Boucherez, J. B. Thibaud, and H. Sentenac. 2001. Guard cell inward K^+ channel activity in *Arabidopsis* involves expression of the twin channel subunits KAT1 and KAT2. *J. Biol. Chem.* 276:3215–3221.

Pilot, G., R. Pratelli, F. Gaymard, Y. Meyer, and H. Sentenac. 2003b. Five-group distribution of the Shaker-like K^+ channel family in higher plants. *J. Mol. Evol.* 56:418–434.

Rodriguez-Navarro, A., and J. Ramos. 1984. Dual system for potassium transport in Saccharomyces cerevisiae. *J. Bacteriol.* 159:940–945.

Ros, R., G. Lemaillet, A. G. Fonrouge-Desbrosses, P. Daram, M. Enjuto, J. M. Salmon, J. B. Thibaud, and H. Sentenac. 1999. Molecular determinants of the *Arabidopsis* AKT1 K^+ channel ionic selectivity investigated by expression in yeast of randomly mutated channels. *Physiol. Plant.* 105:459–468.

Schmitt, N., M. Schwarz, A. Peretz, I. Abitbol, B. Attali, and O. Pongs. 2000. A recessive C-terminal Jervell and Lange-Nielsen mutation of the KCNQ1 channel impairs subunit assembly. *EMBO J.* 19:332–340.

Sentenac, H., N. Bonneaud, M. Minet, F. Lacroute, J. M. Salmon, F. Gaymard, and C. Grignon. 1992. Cloning and expression in yeast of a plant potassium ion transport system. *Science*. 256:663–665.

Tu, L., and C. Deutsch. 1999. Evidence for dimerization of dimers in K^+ channel assembly. *Biophys. J*. 76:2004–2017.

van der Ven, P. F., S. Wiesner, P. Salmikangas, D. Auerbach, M. Himmel, S. Kempa, K. Hayess, D. Pacholsky, A. Taivainen, R. Schroder, O. Carpen, and D. O. Furst. 2000. Indications for a novel muscular dystrophy pathway. Gamma-filamin, the muscle-specific filamin isoform, interacts with myotilin. *J. Cell Biol*. 151:235–248.

Very, A. A., and H. Sentenac. 2002. Cation channels in the *Arabidopsis* plasma membrane. *Trends Plant Sci*. 7:168–175.

Very, A. A., and H. Sentenac. 2003. Molecular mechanisms and regulation of K^+ transport in higher plants. *Annu. Rev. Plant Physiol. Plant Mol. Biol*. 54:575–603.

Wainger, B. J., M. DeGennaro, B. Santoro, S. A. Siegelbaum, and G. R. Tibbs. 2001. Molecular mechanism of cAMP modulation of HCN pacemaker channels. *Nature*. 411:805–810.

Zagotta, W. N., N. B. Olivier, K. D. Black, E. C. Young, R. Olson, and E. Gouaux. 2003. Structural basis for modulation and agonist specificity of HCN pacemaker channels. *Nature*. 425:200–205.

Zimmermann, S., S. Hartje, T. Ehrhardt, G. Plesch, and B. Mueller-Roeber. 2001. The K^+ channel SKT1 is co-expressed with KST1 in potato guard cells–both channels can co-assemble via their conserved K_T domains. *Plant J*. 28:517–527.